Dependence of the structural relaxation of amorphous silicon on implantation temperature

J.-F. Mercure, R. Karmouch, Y. Anahory, S. Roorda, and F. Schiettekatte*
Regroupement Québécois sur les Matériaux de Pointe (RQMP), Département de Physique, Université de Montréal, Case Postale 6128 succ. centre-ville, Montréal, Québec, Canada H3C 3J7
(Received 6 December 2004; published 19 April 2005)

The structural relaxation of amorphous silicon, created by ion implantation, was investigated by *in situ* differential scanning nanocalorimetry. Nanocalorimetry provided the possibility to measure the heat released by relaxation during annealing, for a wide range of implantation fluences and beginning at cryogenic temperatures. Ion implantation was first carried out for fluences between 10^{-5} and 0.8 displacements per atom (DPA) at 133 K and 297 K, and then for temperatures ranging from 118 K to 463 K for fluences of 0.0185 and 0.37 DPA. A heat release saturation occurred above 0.1 DPA, and was found to depend on implantation temperature. The saturation level was extrapolated to 0 K, leading to an estimate of 28 ± 3 kJ/mol for the maximum enthalpy that can be stored in *a*-Si, relative to crystalline Si.

DOI: 10.1103/PhysRevB.71.134205 PACS number(s): 61.43.Dq

I. INTRODUCTION

Amorphous silicon (*a*-Si) continues to generate fundamental interest as it is the prototypical representation of a continuous random network (CRN). It has been studied extensively over the years,[1–11] but a clear understanding of its properties is still missing. A technological interest also exists, as hydrogenated amorphous silicon (*a*-Si:H) is a semiconductor that can be doped and made into thin films, and used in applications such as solar cells and low cost electronics.

Many properties of glasses and amorphous materials depend on their thermal history and their preparation. Most of those properties have the common particularity of being very well defined for the crystalline counterpart of the material. Among these are the electrical conductivity,[7] the density,[1] the melting temperature,[3] the phonon spectrum,[1,10] and the density of states.[12] It is usually said that these properties depend on the state of relaxation.

The structure of *a*-Si is that of a CRN of atoms having a coordination of almost 4. The structure is locally very similar to crystalline silicon (*c*-Si), but is completely disordered at larger scales. The bond length, as measured by x-ray diffraction, is the same as for *c*-Si,[6] but the angles between them are distorted from the tetrahedral diamond structure. The distribution of these distortions ranges between 7° and 12° and varies with the state of relaxation.[1] With these distortions, as well as with broken or dangling bonds, is usually associated a stored enthalpy, $\Delta H = H_{a\text{-Si}} - H_{c\text{-Si}}$, that can be released by annealing, throughout the relaxation process and then by crystallization. In the past, ΔH was evaluated using differential scanning calorimetry (DSC).[2] Ultrapure *a*-Si was produced by means of high-dose ion implantation at 77 K and the DSC experiment was made by scanning between room temperature (RT) and 975 K. The total heat release of $\Delta H = 18.8$ kJ/mol includes $\Delta H_{\text{cryst}} = 13.7$ kJ/mol associated with crystallization around 950 K, yielding $\Delta H_{\text{rel}} = 5.1$ kJ/mol for the relaxation, uniformly released between 413 K and 873 K.

In this paper, relaxation of self-implanted *a*-Si is explored, using *in situ* differential nanocalorimetry. It gives us the possibility to observe the relaxation of *a*-Si at temperatures much lower than RT, revealing a dependence on the implantation temperature of the amount of released heat over the full temperature scan range.

II. EXPERIMENTAL PROCEDURES

A. General principle

Nanocalorimetry provides extremely high sensitivity, of the order of a nanojoule, and allows measurements to be made *in situ*, in the same environment and temperature as for the ion implantation, for instance. It has been used to study melting point depression in nanostructures,[13,14] glass transitions in polymers,[15] liquids,[16] and defects in polycrystalline silicon.[17] The technique is extensively described in Refs. 18 and 19.

A nanocalorimeter consists of a 150-nm-thick low-stress Si_3N_x membrane supporting a 25-nm-thick, 500-μm-wide Pt metallic strip. By measuring the current I flowing through and the voltage drop V across the Pt strip, both the power (VI) and the resistance (V/I) can be calculated. The latter gives the temperature, thanks to a calibration $R(T)$ of the resistance as a function of temperature.[18,20] Heating rates of up to 10^6 K/s confer on the technique an extremely high sensitivity.

For these experiments, a 140 nm layer of *a*-Si was deposited by Ar plasma sputtering (base pressure 3×10^{-5} Pa) on the nitride membrane of both sample and reference calorimeters. The material was deposited at a rate of 2.3 Å/s with a shadow mask, in line with the Pt strip but on the opposite side of the membrane. The width of the *a*-Si layer was actually 650 μm, exceeding the width of the Pt strip by 75 μm on each side. The issue of the layer width and uniformity has been addressed in another paper[20] and turns out to be of minor influence. Meanwhile, we included in our analysis an uncertainty of 15% on the area of deposited *a*-Si. This induces a systematic error on the measurements, but the relative error between each measurement is much smaller. The calorimeters were then annealed to 773 K for 10 s, and an-

nealed again for a few hours during the calibration procedure described below. Resulting layers contained 1% Ar and 3% H.

B. Ion Implantation

One and the same sample could be used repeatedly for different fluences and implantation temperatures. Temperature scans were performed by heating up to 775 K, just below recrystallization, so the relaxed state of *a*-Si is obtained at the end of each scan. As these operations were carried out *in situ*, we were thus able to cyclingly "unrelax" the sample by self-implantation, and then measure the heat released by relaxation during a nanocalorimetry scan.

Ion implantation was performed using a 1.7 MV Tandetron accelerator in acceleration-deceleration mode. Si^- ions with an energy of 30 keV were used to unrelax the *a*-Si thin film on the sample calorimeter, while the reference was hidden from the beam. Such low-energy ions will not traverse the *a*-Si and reach the Si_3N_x. This is confirmed by the fact that no change in sample nanocalorimeter resistance was detected, at RT, after irradiation. The currents used ranged between 300 and 500 nA, over an area of 17.22 cm^2, delivering 30 μW to the nanocalorimeter strip, which is three orders of magnitude smaller than the power supplied during a temperature scan. Ion implantation was carried out at different sample temperatures and fluences, first with fluences between 0.001 and 4 Si/nm^2, corresponding to 2×10^{-4} and 0.8 DPA (displacements per atom), according to SRIM 2000 simulations,[21] at 133 K and RT, and then with two fluences, 0.1 and 2 Si/nm^2 (0.0185 and 0.37 DPA), at temperatures ranging between 118 and 463 K. For fluences higher than 0.1 DPA, the heat release saturates. The uncertainty on the fluence is of about 10%.

C. Nanocalorimetry

Prior to experiments, the resistance $R(T)$ and the power of heat losses $P(T)$ as functions of temperature of the nanocalorimeters were determined. The heater strip resistance $R(T)$ was calibrated against temperature using a four-point resistance measurement, during slow cooling between 725 K and RT in a quartz furnace, under flowing nitrogen, and slow heating from 185 K to RT in a cold bath of acetone. In order to remain close to thermal equilibrium, the temperature was varied very slowly, the whole process lasting over 12 h. The calibration was extrapolated from 100 to 775 K for data analysis, using the known temperature dependence of the Pt resistivity.[20] The heat loss function $P(T)$ is evaluated using baselines acquired with different heating rates, as described in Ref. 22.

The nanocalorimeters were installed on a sample holder supporting a copper thermal shield, which can be cooled to 110 K. A small hole in the thermal shield allowed the beam to reach the sample nanocalorimeter. The large thermal mass of the sample holder and thermal shield ensured that the temperature around the nanocalorimeter varied only very slowly. For *in situ* measurements, the calorimeter holder assembly was put in the ion implantation chamber maintaining a vacuum of better than 10^{-4} Pa. The ion beam heated the sample by between 4 K and 10 K, as measured by resistivity during implantation. The nanocalorimetry scans were carried out between the temperature at which the sample was irradiated and 775 K, and all lasted 15 ms. Heating rates around 40 000 K/s were used. Care was taken not to heat above 800 K so as to avoid the onset of crystallization.

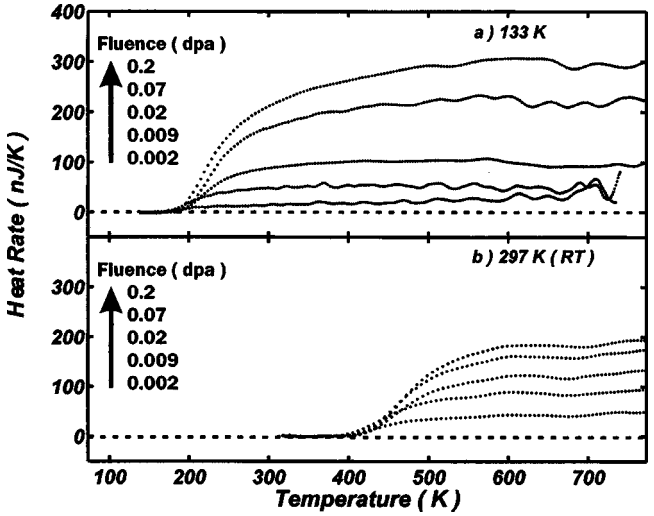

FIG. 1. Heat release curves for different implantation fluences at (a) 133 K and (b) RT. The scaling is the same for both sets of curves.

The heat released by *a*-Si relaxation was always detected on the first nanocalorimetry scan after ion implantation, and no heat was detected during subsequent scans, the latter being identical to the baseline measurements taken before irradiation. The calculation used to extract the heat release from *V* and *I* measurements is based on the method developed by Efremov *et al.*[22] and summarized in Ref. 20. It takes into account the difference in temperature and heating rate between the experiment and baseline scans.

III. NANOCALORIMETRY RESULTS

A. Heat releases and fluence

Figure 1 shows a few curves for the heat releases at fluences between 0.01 and 1 Si/nm^2, corresponding to 0.002 and 0.2 DPA, for ion implantation at 133 K (top) and RT (bottom). The data were all taken on the same sample and have been filtered to remove high-frequency noise, for a clearer view, but no structure that can be associated with physical phenomena was lost in the process. A random dc offset, always smaller than 15 nJ/K, was removed so that the signal starts at zero. This offset is produced by the differential voltage amplifier.[19] The average heating rates were of 43 000 K/s for the 133 K data and 32 000 K/s for RT. We were able to detect a heat signal for fluences from 2×10^{-5} to 0.8 DPA.

All the curves have the same shape, although not the same amplitude. The heat release is fairly constant, up to 773 K in both cases, although it starts at a much lower temperature for the 133 K implantations. In this way, low-temperature mea-

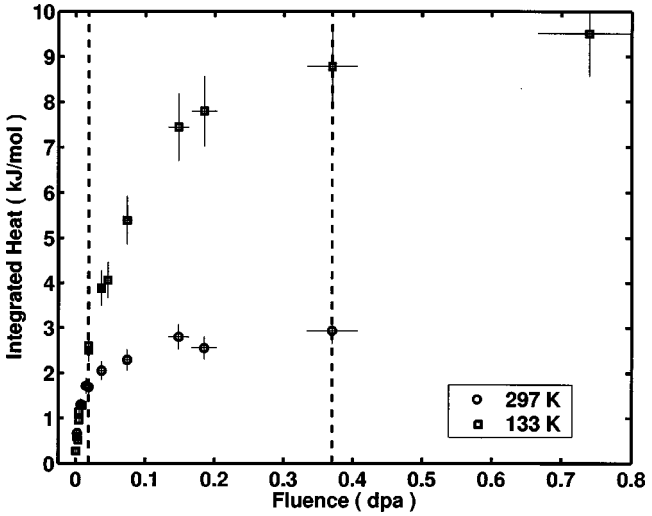

FIG. 2. Heat integrated between 113 K and 773 K vs implantation fluence. The squares are for 133 K implantations and the circles for 297 K. The error bars account for the uncertainty in the evaluation of $P(T)$, the heat losses, and for the implantation fluence.

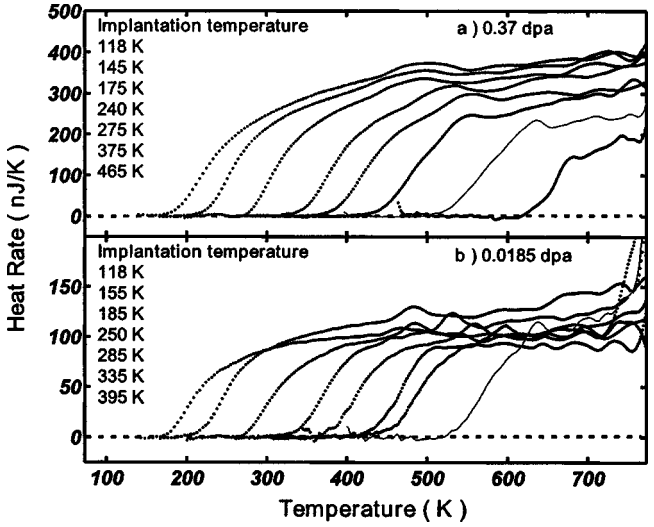

FIG. 3. Heat releases for implantations at different temperatures, following the order of the curves, for fluences of (a) 0.37 DPA, in the saturated regime, and (b) 0.0185 DPA, well below saturation fluence.

surements follow the same trend as previously measured in DSC experiments starting at RT.[1] In Fig. 1, the fluence increases exponentially, while the amplitude does not, revealing a saturation. This saturation can be observed in Fig. 2, where the integrated heat rate between 113 K and 773 K is plotted in kJ/mol for all fluences and both implantation temperatures. It is clear that above a fluence corresponding to 0.1 DPA, the nanocalorimetry curve amplitude changes only slightly. It is also seen that the integrated amounts of heat do not reach the same saturation value at high fluence.

B. Heat releases and implantation temperature

In order to clarify the temperature-dependent saturation, measurements were carried out at several implantation temperatures for a low and a high fluence, 0.0185 and 0.37 DPA, respectively. These fluences are indicated by dashed lines in Fig. 2. Figure 3 shows the resulting heat releases, measured on a second sample nanocalorimeter. The amount of *a*-Si can differ slightly from the first sample. The implantation temperatures were always measured from the initial value of a nanocalorimetry scan, to which we added an estimate of the beam heating, between 4 and 10 K. The amplitude of the curves decreased with implant temperature for implantations in the saturated regime (0.37 DPA), which was not the case for implantations below saturation fluences (0.0185 DPA). The integrated heat of these curves is plotted in Fig. 4 for both fluences. The relation is almost linear. Two effects contribute to reduce the heat release as the implantation temperature is increased: the decreasing amplitude and the increasing onset temperature. For the saturated case, both effects take place, while only the second holds for undersaturated implants.

Let us now make explicit the two contributions. In Fig. 5, we show the onset temperature where the heat release exceeds 10 nJ/K. The onset temperature increases linearly with implantation temperature, with a ratio of 1.33 ± 0.05, for both sets of data. It is the dominant contribution for the variation of the integrated heat of Fig. 4. However, the relationship is different for the amplitude. The averaged amplitude, that is, the heat rate during the plateau phase of the heat release, is plotted in Fig. 6. A clear decrease is noticed for the saturation fluence, while the average amplitude is independent of the implantation temperature for low fluence implants, as we already observed in Fig. 3. The implantation temperature effect is a new aspect of the relaxation phenomenon revealed by these data. Previous work showed heat flowing at the same amplitude for *a*-Si annealed at different temperatures,[1] but samples were always implanted at the same temperature.

The high fluence amplitudes are characterized by a saturation towards 0 K. A second-order polynomial was fitted to

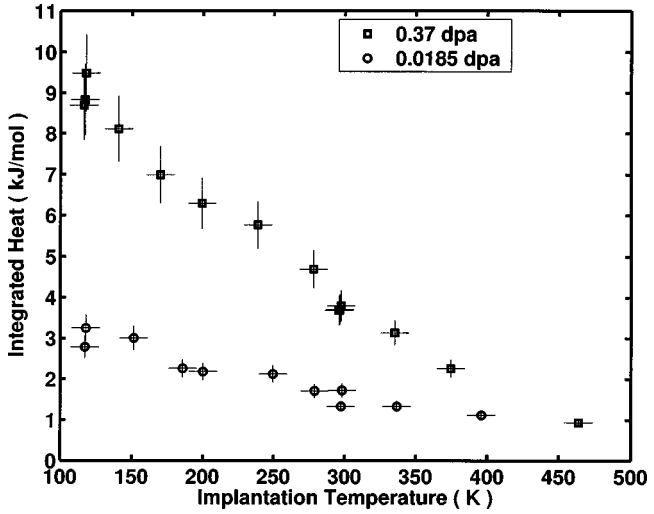

FIG. 4. Heat integrated between −113 K and 773 K vs implantation temperature, for the saturated regime (squares) and not saturated (circles). The error bars account for the uncertainty in $P(T)$, as in Fig. 2, and that on the beam heating.

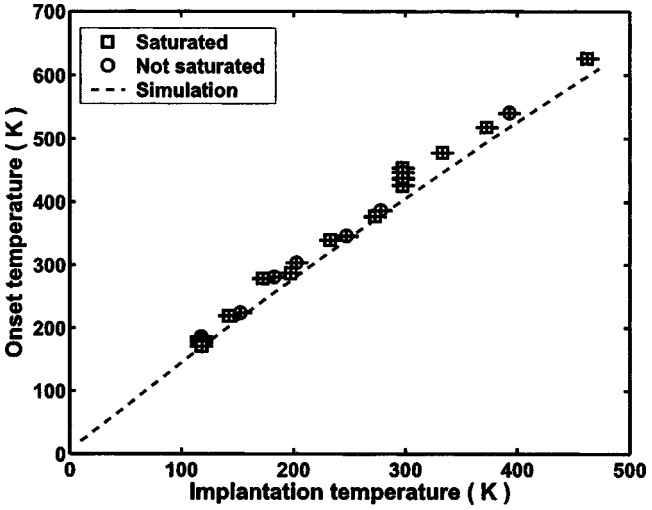

FIG. 5. The temperature at which the heat rate is greater than 10^{-8} J/K, vs the implantation temperature, for the high fluences (squares) and the low (circles). The dashed line is calculated using the model described in Sec. IV A.

these data. The linear part of the fit is very small and the parabola is almost centered at 0 K. Extrapolation of the dashed curve to 0 K would give the maximum amount of energy that can be stored in *a*-Si even at 0 K. Considering this extrapolation, the total heat release for a 0 K ion implantation and a scan from that temperature to 773 K would yield 14.6 kJ/mol. In this case, the heat release would increase instantly from zero to 400 nJ/K at 0 K, and remain constant towards crystallization.

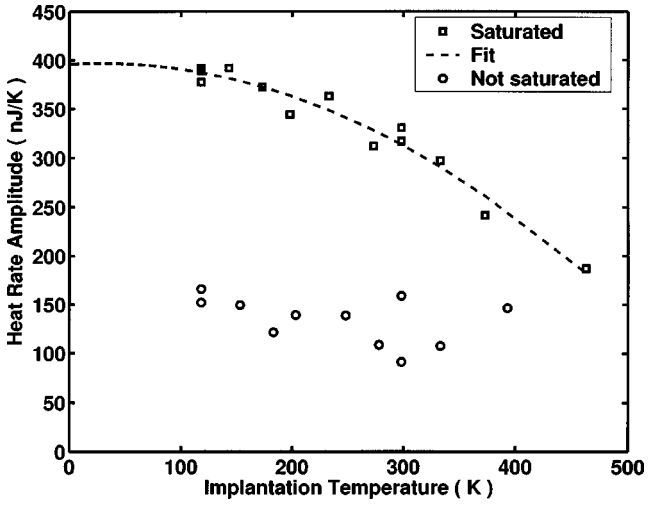

FIG. 6. Heat rate amplitude, averaged between 723 K and 773 K, for the high fluences (squares) and the low (circles). The dashed line is a polynomial fit of second order, of which the linear part is very small. It approaches the value 400 nJ/K. No tendency is seen in the low fluence data.

IV. DISCUSSION: THE EQUILIBRIUM STATE OF RELAXATION

A. Activation energy spectrum

The data in Fig. 5 can be understood with a model based on a theory of structural relaxation by Gibbs,[23] extended to include second-order kinetics. Roorda demonstrated that differential isothermal calorimetry curves of the relaxation in ion implanted *a*-Si exhibit bimolecular reaction kinetics.[1] If we interpret the energy released during a scan with the annealing of a continuously distributed density of two-level processes, $n(\varepsilon)$, each with an activation energy ε, then the number of transitions from the higher level to the lower, during a time interval dt, is

$$dn(\varepsilon,t) = -n^2(\varepsilon,t)V_0 v_0 \exp\left(-\frac{\varepsilon}{kT}\right)dt, \tag{1}$$

where v_0 is the frequency of the order[7] $10^{12}-10^{14}\mathrm{s}^{-1}$ and V_0 is the volume of interaction between the processes, which we estimate of the order $0.1-1\ \mathrm{nm}^{-3}$. Since the calorimetry curves are very flat along temperature, we use a constant initial density of processes n_0. The experimental procedure requires an isothermal (dynamic) anneal of 30s, and then a nanocalorimetry scan. The remaining density after the first is simply the integration in time of Eq. (1),

$$n(\varepsilon,t) = \frac{n_0}{1 + n_0 v_0 V_0 t \exp\left(\frac{-\varepsilon}{kT}\right)}. \tag{2}$$

This is a steplike function, the derivative of which, in ε, is Gaussian-like and of width increasing linearly with T. Its maximum travels along ε with $\log(t)$ and depends linearly on T, so that the difference in the anneal temperature and that at which heat starts to flow increases with the time between the implantation and the scan, as $\log(t)$, but also linearly with anneal temperature T.

For the scan, the calculation cannot be done analytically, as we need to use the function $T(t)$, which is not completely linear for nanocalorimetry, because of heat losses increasing with T, and we have to perform the calculation numerically. If each process releases the same amount of energy, h_0, then the heat released during a scan would be

$$\frac{dH(T)}{dT} = \int_0^\infty h_0 V_0 \frac{dn(\varepsilon,T)}{dT} d\varepsilon, \tag{3}$$

with $T(t)$ being a monotonically increasing function in time. From this model, we can calculate the onset temperature. The results are plotted in Fig. 5 (dashed line). They are, as expected, nearly linear with an average slope of 1.28.

This model can explain the onset temperature and the plateau observed in the heat release, but suggests no mechanism to explain the dependence seen in Fig. 6. This would require a change in the constant initial density of processes n_0 with the implantation temperature at which the unrelaxation occurs.

One way to describe the phenomenon accounting for the changing amplitude is to regard the process as if the system, upon implantation, scales a nonuniform multilevel ladder in terms of energy associated to structural configurations, sche-

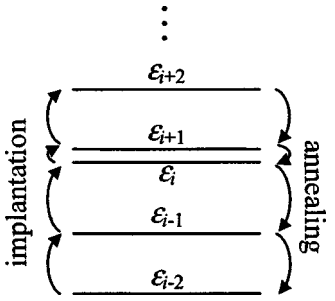

FIG. 7. Schematic representation of the configurational energy levels during ion implantation and relaxation.

matically represented in Fig. 7. At 0 K, the system just climbs the ladder until it reaches absolute saturation. But at finite implantation temperature, the system reaches states for which relaxation can be easily thermally activated (e.g., level ε_{i+1} in Fig. 7), preventing it from reaching subsequent levels and storing energy. Consequently, as the temperature decreases, new configurations build up that could not exist if underlying, low activation energy configurations were allowed to dynamically relax during implantation.

B. Gibbs free energy

As mentioned previously, the extrapolation of Fig. 6 towards 0 K suggests that there is a maximum in the energy that can be stored in an amorphous network, and this maximum would be obtained by performing ion implantation at 0 K. This maximum enthalpy would then correspond to that of relaxation plus that of crystallization, for a total of 28 ± 3 kJ/mol (the uncertainty includes that of the amount of deposited material). We then conclude that no quasiequilibrium relaxation state can exist with a larger stored enthalpy. Figure 8 sketches the Gibbs free-energy difference between *a*-Si and *c*-Si. The curve for fully relaxed *a*-Si was calculated using[3]

$$\Delta G(T) = H_0 - TS_0 + \int_0^T C_p(T')dT' - T\int_0^T \frac{C_p(T')}{T'}dT', \tag{4}$$

where $C_p(T)$ is the heat capacity of the *a*-Si, H_0 is the enthalpy of crystallization, and S_0 is the configurational entropy. The values are the same as those used by Donovan *et al.*[5] except H_0, for which we took the value of crystallization enthalpy measured by Roorda, 13.7 kJ/mol. The curves of $\Delta G(T)$ for unrelaxed states of *a*-Si at the saturation (dotted lines) were constructed assuming that no additional relaxation occurs, and correspond to that of relaxed *a*-Si with an additionnal constant contribution to ΔG, calculated using the integrated heat data from Fig. 4, for the saturated regime at 133 K and RT. The thick curve on top is the same, considering the extrapolated additional contribution of 14.6 kJ/mol at 0 K. With the boundary given by $\Delta G(T)$ for the liquid state, there is a limited region where *a*-Si can exist, shown by the shaded region.

Amorphous Si in the shaded region is not completely stable for all ΔG and T at longer time scales. The dashed lines represent the path followed during relaxation. From any equilibrium relaxation state, the system would follow $\Delta G(T)$ at any temperature lower than the implantation temperature and would diverge from it at higher temperatures, until it reached that for relaxed *a*-Si, and then crystallization would occur. The different slopes reflect the change in heat rate amplitude with unrelaxation temperature. In the case where *a*-Si would be unrelaxed by implantation at 0 K, the relaxation process would begin immediatly, following the top dashed line. When *a*-Si is allowed to relax, the relaxation states are limited by the shaded region under that path.

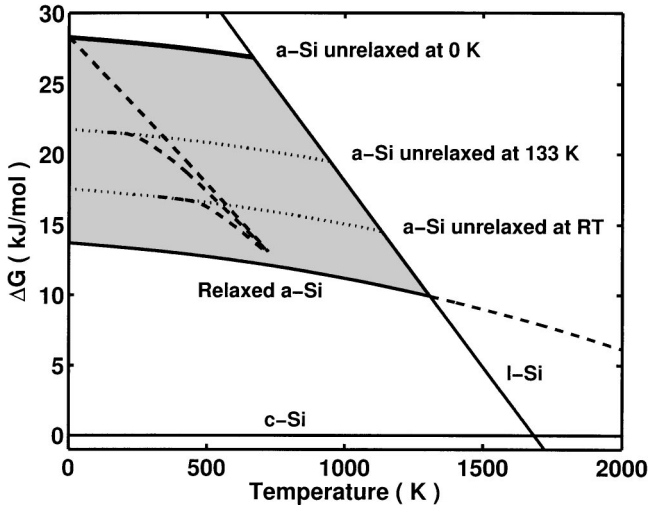

FIG. 8. Approximate calculation of the Gibbs free energy for different states of relaxation of *a*-Si, relative to that of *c*-Si. The curve starting with an enthalpy H_0 at 0 K of 13.7 kJ/mol represents the completely relaxed state, which corresponds to the enthalpy of crystallization, and was calculated using the method of Donovan *et al.* (Ref. 5) as was the curve for *l*-Si. The thick curve on top represents the maximum unrelaxed state, using the extrapolated enthalpy $H_0=13.7+14.6=28.3\pm2.9$ kJ/mol. The gray region then limits the possible partially relaxed states of *a*-Si. The dashed curves are the paths followed by relaxation during a nanocalorimetry scan, starting at different relaxation states, sketched by the dotted lines. The top one is a virtual process starting at 0 K, while the other two are actual data from the nanocalorimetry scan for saturated systems.

In an extension of the model proposed by Roorda *et al.*,[3] for which each quasiequilibrium relaxation state resulted from annealing to a specific temperature after ion implantation, we observe here two parameters upon which enthalpy depends: the annealing temperature and the implantation temperature. For example, a sample implanted at a low temperature T_1 and then annealed to a second T_2 could contain the same stored enthalpy as one implanted at another temperature T_3, such that $T_1<T_3<T_2$. The thermal processes activated during a nanocalorimetry scan would not be the same, but the total heat released would be. A low-temperature ion implantation, in the saturated regime, results in a greater number of high activation energy processes than at RT.

C. Raman TO-like peak half-width

The enthalpy of relaxation $H_{\mathrm{rel}}=H-H_0$ can be linked to the half-width of the Raman TO-like peak ($\Gamma/2$), the latter

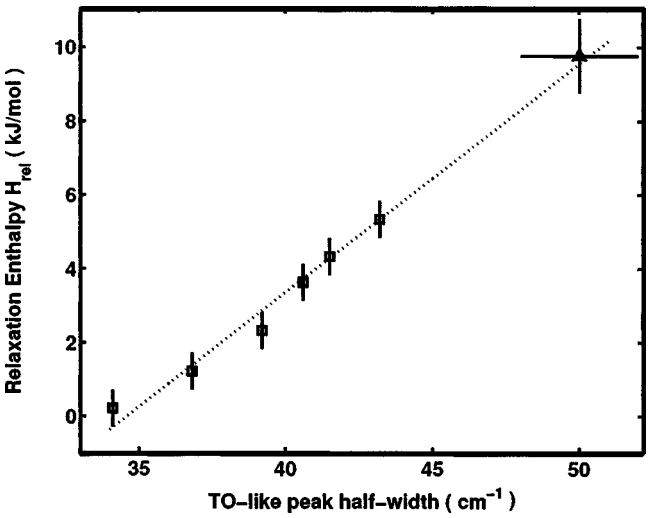

FIG. 9. Relaxation enthalpy H_{rel} as a function of the TO-like peak half-width of the Raman spectrum of *a*-Si ($\Gamma/2$). The data in squares, which were taken by Roorda (Ref. 1), is for *a*-Si implanted at 77 K and annealed at different temperatures between 300 and 500 K. The triangle represents a new data point : the Raman peak half-width was measured by Coffa (Ref. 10) with an *in situ* apparatus, for implantation and measurement at 77 K, while we extrapolated the enthalpy from our data. The dashed line is a linear fit.

being associated with the width of the bond angle distribution. H_{rel} can be extrapolated linearly to 77 K from Fig. 4. Correspondingly, Coffa *et al.* measured $\Gamma/2=50\pm2$ cm^{-1} at this temperature.[10] This point is represented as a triangle in Fig. 9. It falls in excellent agreement with previous measurement by Roorda[1] carried out at RT after amorphizing by self-implantation at liquid nitrogen temperature, and annealing further at different temperatures; the width varies between 34 and 44 cm^{-1}. He proposed a linear relation between H_{rel} and $\Gamma/2$, although a linear relation between $\sqrt{H}$ and $\Gamma/2$ could also be valid, where H is the total enthalpy. The new data point supports the first relation proposed, but cannot rule out the second as that relation is almost linear in the relatively short enthalpy range in which the measurement extends. By linear extrapolation of the data in Fig. 9 toward a maximum enthalpy of 14.6 kJ/mol, we calculated that for an implantation at 0 K, $\Gamma/2$ could become as large as 60 cm^{-1}.

The total maximum enthalpy, including recrystallization energy, can also be used to estimate the maximum width for the bond angle distribution $\Delta\theta$ at 0 K. Laaziri *et al.*[24] measured $\Delta\theta$ values of 10.4° and 9.6° for as-implanted samples ($H=19.0$ kJ/mol) and fully relaxed *a*-Si ($H=13.9$ kJ/mol), repectively. Considering a relation[25] of the type $H\sim\Delta\theta^2$, it would mean that $\Delta\theta=12.0\pm0.5°$ at 77 K ($H=23.3$ kJ/mol), and its maximum possible value should be $13.2\pm0.5°$ at 0 K ($H=28.3$ kJ/mol). These values compare fairly well to recent simulations.[11]

V. CONCLUSION

In summary, we have studied by nanocalorimetry the process of relaxation in *a*-Si following ion implantation under different implantation temperatures. For all implantation temperatures, there was a saturation fluence above which no more unrelaxation is possible in the material, and there was a dependence on the amount of released heat with the implantation temperature. The onset temperature at which, during annealing, heat starts to be released is a linear function of implantation temperature. This is explained by a model considering the activation of a continuously distributed density of two-level processes. The saturation amplitude of the nanocalorimetry curves also depends on the implantation temperature, and tends towards a maximum amount for unrelaxation at 0 K, which determines that the maximum enthalpy that can be stored in the amorphous network is 28 ± 3 kJ/mol. The implantation temperature and the annealing temperature will determine the quasiequilibrium relaxation state and enthalpy of *a*-Si, a larger number of unrelaxed configurations being created at low temperature on the basis of low-energy states surviving dynamic annealing during the implantation. Finally, by extrapolation of these measurements, we provide a relation between the relaxation enthalpy and the half-width of the Raman TO-like peak after implantations at 77 K. These new data are in excellent agreement with the linear relation proposed previously between the heat of relaxation and the half-width.

ACKNOWLEDGMENTS

The authors are grateful to N. Mousseau (U. Montréal) and L. H. Allen and M. Yu. Efremov (UIUC) for fruitful discussions. Thanks are also due to L. Godbout and R. Gosselin for their excellent technical assistance with the accelerator operation, and M. Skvarla and P. Infante of the Cornell Nanofabrication Facility, as well as O. Grenier and S. Bah of the École Polytechnique de Montréal for their assistance with nanocalorimeters fabrication. This work benefited from the financial support of NanoQuébec, the Fonds Québécois de Recherche sur la Nature et les Technologies, and the Natural Science and Engineering Research Council of Canada.

*Electronic address: francois.schiettekatte@UMontreal.ca

[1] S. Roorda, W. Sinke, J. Poate, D. Jacobson, S. Dierker, B. S. Dennis, D. J. Eaglesham, F. Spaepen, and P. Fuoss, Phys. Rev. B **44**, 3702 (1991).

[2] S. Roorda, S. Doorn, W. Sinke, P. Scholte, and E. van Loenen, Phys. Rev. Lett. **62**, 1880 (1989).

[3] W. Sinke, S. Roorda, and F. Saris, J. Mater. Res. **3**, 1201 (1988).

[4] S. Roorda, R. Hakvoort, A. van Veen, P. Stolk, and F. Saris, J. Appl. Phys. **72**, 5145 (1992).

[5] E. Donovan, F. Spaepen, D. Turnbull, J. Poate, and D. Jacobson,

Appl. Phys. Lett. **42**, 698 (1983).
[6] K. Laaziri, S. Kycia, S. Roorda, M. Chicoine, J. L. Robertson, J. Wang, and S. C. Moss, Phys. Rev. Lett. **82**, 3460 (1999).
[7] J. H. Shin and H. A. Atwater, Phys. Rev. B **48**, 5964 (1993).
[8] M. G. Grimaldi, P. Baeri, and M. A. Malvezzi, Phys. Rev. B **44**, 1546 (1991).
[9] F. Valiquette and N. Mousseau, Phys. Rev. B **68**, 125209 (2003).
[10] A. Battaglia, S. Coffa, F. Priolo, G. Compagnini, and G. A. Baratta, Appl. Phys. Lett. **63**, 2204 (1993).
[11] P. Biswas, R. Atta-Fynn, and D. A. Drabold, Phys. Rev. B **69**, 195207 (2004).
[12] S. Coffa, F. Priolo, and A. Battaglia, Phys. Rev. Lett. **70**, 3756 (1993).
[13] M. Y. Efremov, F. Schiettekatte, M. Zhang, E. A. Olson, A. T. Kwan, R. S. Berry, and L. H. Allen, Phys. Rev. Lett. **85**, 3560 (2000).
[14] M. Zhang, M. Y. Efremov, F. Schiettekatte, E. A. Olson, A. T. Kwan, S. L. Lai, T. Wisleder, J. E. Greene, and L. H. Allen, Phys. Rev. B **62**, 10 548 (2000).
[15] M. Yu. Efremov, E. A. Olson, M. Zhang, Z. Zhang, and L. H. Allen, Phys. Rev. Lett. **91**, 085703 (2003).
[16] E. A. Olson, M. Y. Efremov, A. Kwan, S. Lai, V. Petrova, F. Schiettekatte, J. T. Warren, M. Zhang, and L. H. Allen, Appl. Phys. Lett. **77**, 2671 (2000).
[17] R. Karmouch, J.-F. Mercure, Y. Anahory, and F. Schiettekatte, Appl. Phys. Lett. **86**, 031912 (2005).
[18] M. Y. Efremov, E. A. Olson, M. Zhang, S. L. Lai, F. Schiettekatte, Z. S. Zhang, and L. H. Allen, Rev. Sci. Instrum. **75**, 179 (2004).
[19] J.-F. Mercure, R. Karmouch, Y. Anahory, S. Roorda, and F. Schiettekatte, Physica B **340-342**, 622 (2003).
[20] R. Karmouch, J.-F. Mercure, and F. Schiettekatte, Thermochim. Acta (to be published).
[21] J. F. Ziegler, J. P. Biersack, and U. Littmark, *The Stopping and Ion Range of Ions in Matter* (Pergamon, New York, 1985).
[22] M. Y. Efremov, E. A. Olson, M. Zhang, S. L. Lai, F. Schiettekatte, Z. S. Zhang, and L. H. Allen, Thermochim. Acta **412**, 13 (2004).
[23] M. Gibbs, J. Evetts, and J. Leake, J. Mater. Sci. **18**, 278 (1983).
[24] K. Laaziri, S. Kycia, S. Roorda, M. Chicoine, J. L. Robertson, J. Wang, and S. C. Moss, Phys. Rev. B **60**, 13 520 (1999).
[25] T. Saito, T. Karasawa, and I. Ohdomari, J. Non-Cryst. Solids **50**, 271 (1982).